

# The consequences of tritium mix for simulated ion cyclotron emission spectra from deuterium-tritium plasmas

Tobias Slade-Harajda<sup>1</sup>, Richard Dendy<sup>1</sup>, Sandra Chapman<sup>1,2</sup>

<sup>1</sup> Centre for Fusion Space and Astrophysics, Department of Physics, Warwick University, Coventry CV4

<sup>2</sup> Department of Mathematics and Statistics, University of Tromsø, Norway



This work received support from the RCUK Energy Programme grant no. EP/T012250/1 and was carried out within the framework of the HPC Midlands+ partnership.

## What is Ion Cyclotron Emission (ICE)?

- Strongly suprathermal emission and highly spectrally structured ICRF signal spontaneously emitted from most large MCF plasmas
- Driven by energetic ion populations: fusion-born in deuterium and deuterium-tritium (DT) plasmas, also NBI and occasionally ICRH
- Spectral peaks at local cyclotron harmonics of energetic ion population
- Driven by the magnetoacoustic cyclotron instability (MCI)

- Brought on by strong positive gradients in energetic minority particle's velocity-space distribution
- Originally detected in JET using ICRH antennae used to launch fast Alfvén wave

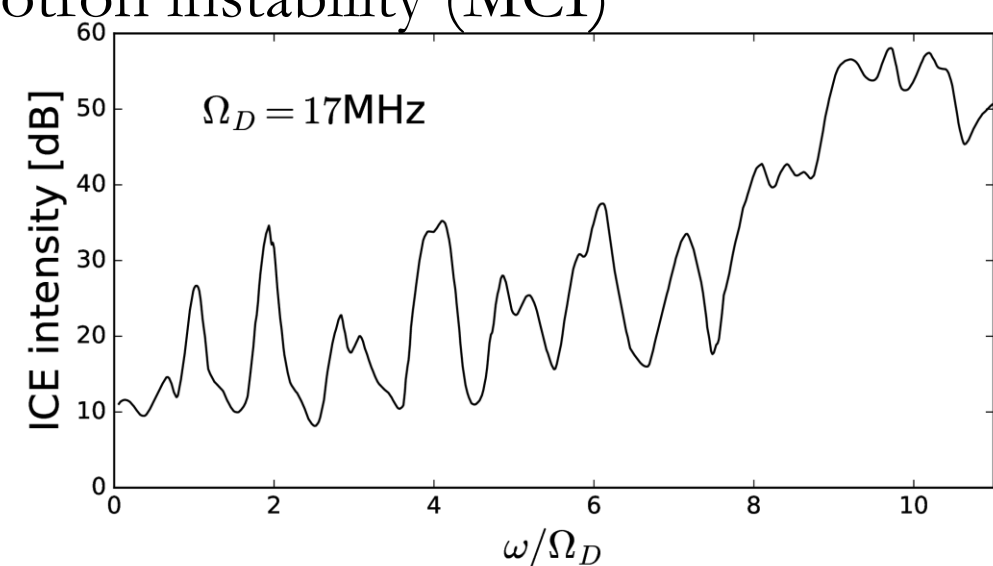


Fig. 1 ICE power spectrum, recreated from [1]. Peaks seen at integer deuterium ion harmonics, for a cyclotron frequency of 17MHz.

## Why do we measure ICE?

- By understanding ICE physics, we can use ICE measurements to infer features of the energetic ion distribution
- Passive and non-intrusive
- Scaled linearly with fusion reactivity in JET
- Observed at various poloidal angles around tokamak
- ICE frequency ranges are typical of antennae already used in tokamaks

## Experimental setup

- ICE is observed from most large MCF plasmas, including JET tokamak [2], Fig. 2, and LHD heliotron-stellarator [3], Fig. 3
- DT fusion reaction considered:  $D + T \rightarrow \alpha + n$  (3.5MeV) +  $e^-$
- Thermal bulk (background) ions (electrons)  $T_{i,e} \sim keV$

Fig. 2 The general tokamak layout, adapted from [4], with the poloidal ( $\theta$ ) and toroidal ( $\phi$ ) magnetic fields as labelled. Poloidal field generated from applied plasma current, producing an overall helical magnetic field, spiralling around the plasma.

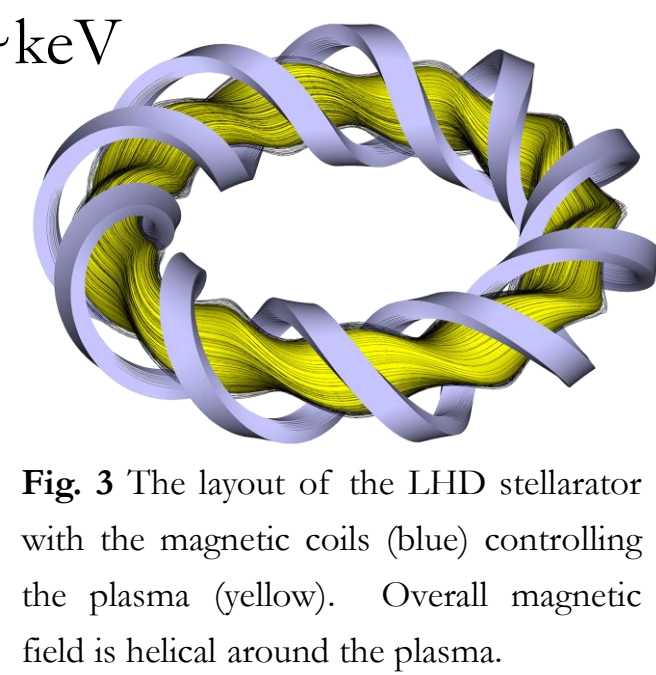
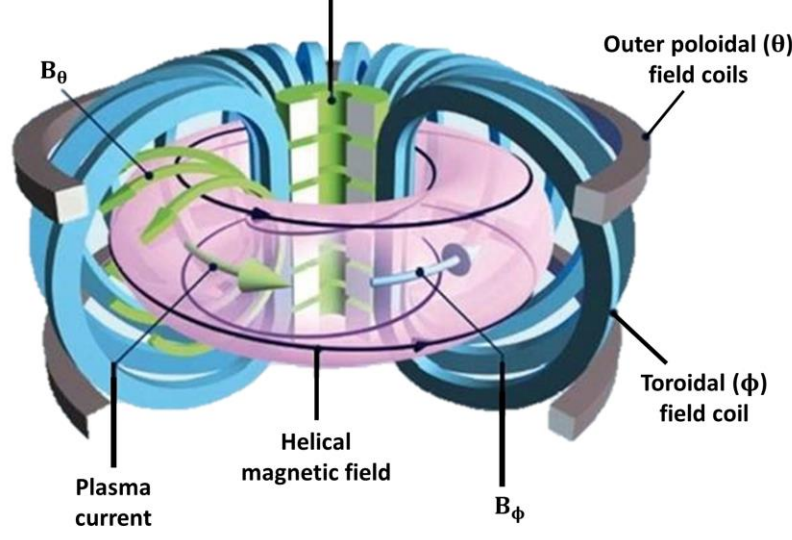


Fig. 3 The layout of the LHD stellarator with the magnetic coils (blue) controlling the plasma (yellow). Overall magnetic field is helical around the plasma.

## Simulation setup & Tritium ion concentration

- 1D3V PIC code EPOCH [5] self consistently evolves Maxwell-Lorentz system of equations
- 3.5MeV  $\alpha$ -particle distributed as ring-beam, eq. (1), where  $\perp$  &  $\parallel$  are w.r.t magnetic field  $B_z$  component

$$f_\alpha(v_\parallel, v_\perp) \propto \exp\left(-\frac{(v_\parallel - v_0)^2}{v_r^2}\right) \exp\left(-\frac{(v_\perp - u_0)^2}{u_r^2}\right) \quad (1)$$

- Particle volumes held equal according to the numerical weighting, eq. (2), to remove linear heating across all species, indexed  $\sigma$ ,

$$\frac{n_\sigma}{N_{s\sigma}} = const \quad (2)$$

- General parameters of the JET 26148 plasma:  $n_e = 10^{19} m^{-3}$ ;  $B_0 = 2.1T$ ;  $B \angle k = 89^\circ$ ;  $T_{i,e} = 1keV$ ;  $n_\alpha/n_e = 2 \times 10^{-3}$

[1] Cottrell G A *et al.* 1993 *Nucl. Fusion* **33** 1365–87  
 [2] McClements K G *et al.* 1999 *Phys. Rev. Lett.* **82** 2099–102  
 [3] Reman B C G *et al.* 2019 *Nucl. Fusion* **59** 096013  
 [4] D. O. E. <https://www.energy.gov/science/doe-explainstokamaks>

[5] Arber T D *et al.* 2015 *Plasma Physics and Controlled Fusion* **57** 113001  
 [6] Naylor T and Jeffries R D 2006 *MNRAS* **373**  
 [7] Dendy R O *et al.* 2023 *Phys. Rev. Lett.* **130** 105102

## Power spectra & Frequency offsets

Using the spatiotemporal Fourier transform of the oscillatory field component,  $\Delta B_z$ , we integrate over a range of wavenumbers,  $k$ , to return the power spectra as a function of frequency, Fig. 4. There are noticeable ICE peaks in all primary traces and a noticeable shifting of the dominant region ( $16 < \omega/\Omega_D < 21$ ) as triton concentration increases.

Using various correlation methods including the cross-correlation, phase-correlation and shared area we defined this frequency shift by a linear relation w.r.t tritium concentration:

$$\omega_{off}/\Omega_D = (-4.74 \pm 0.34) \xi_T + (-0.01 \pm 0.16) \quad (3)$$

Frequency shifts are described as the preferential driving of lower energy waves for heavier, more inertial, plasmas. Best fitting simulated spectra to those in Fig. 1 is that of the 11% case, according to a  $\tau^2$  fitting method [6].

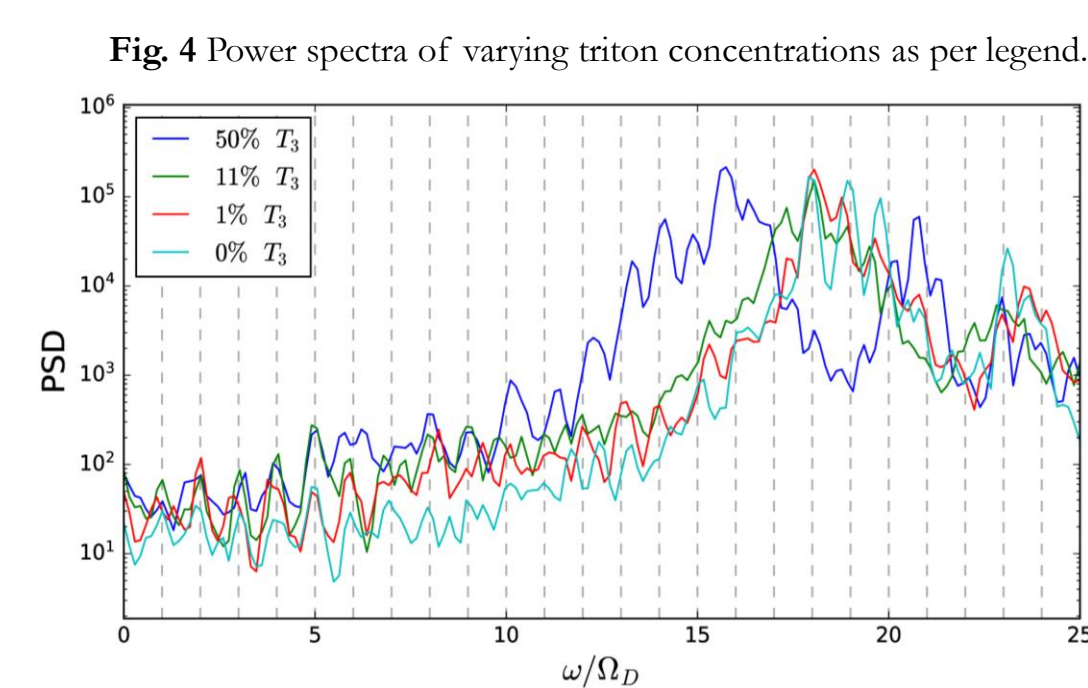


Fig. 4 Power spectra of varying triton concentrations as per legend.

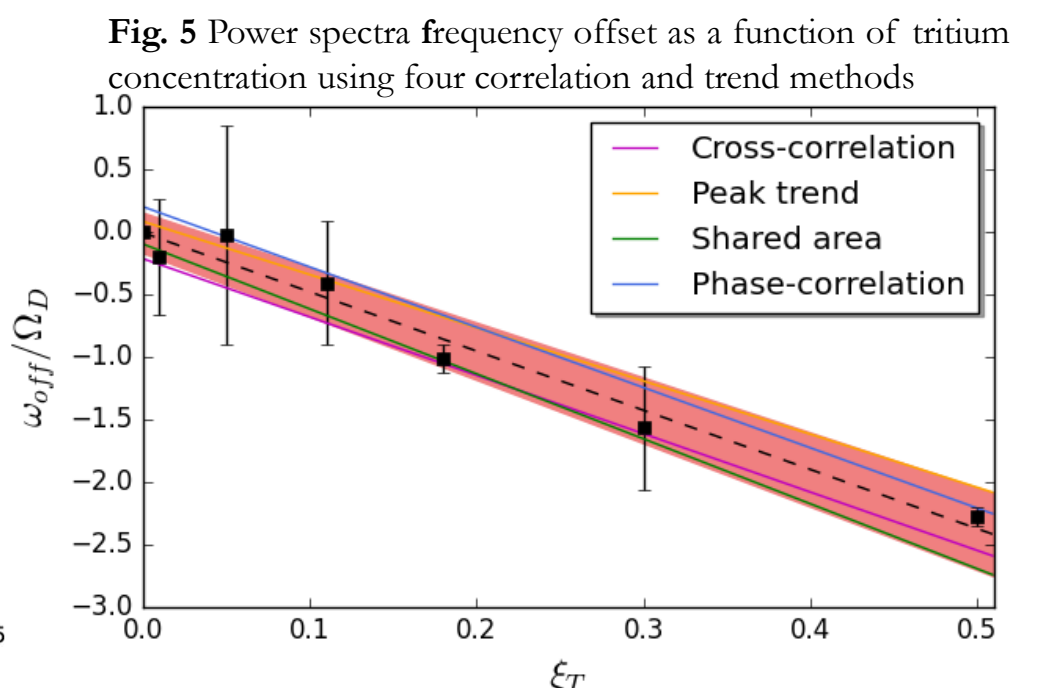


Fig. 5 Power spectra frequency offset as a function of tritium concentration using four correlation and trend methods

## Energy densities & Three-ion species gyro-resonance

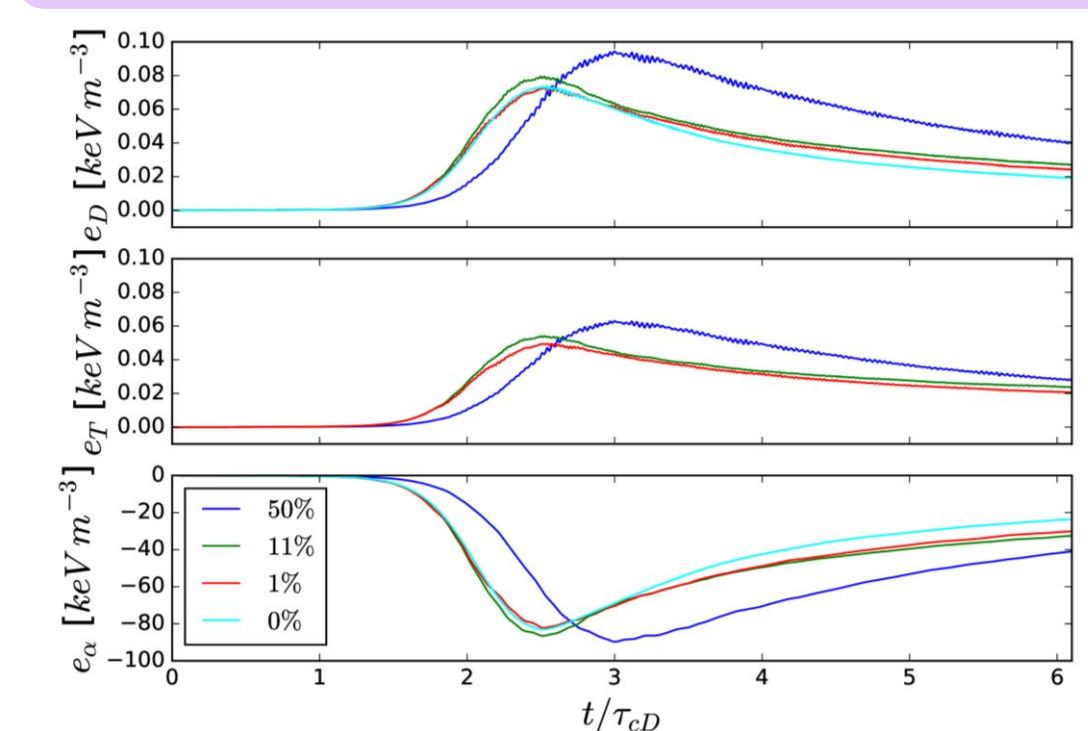
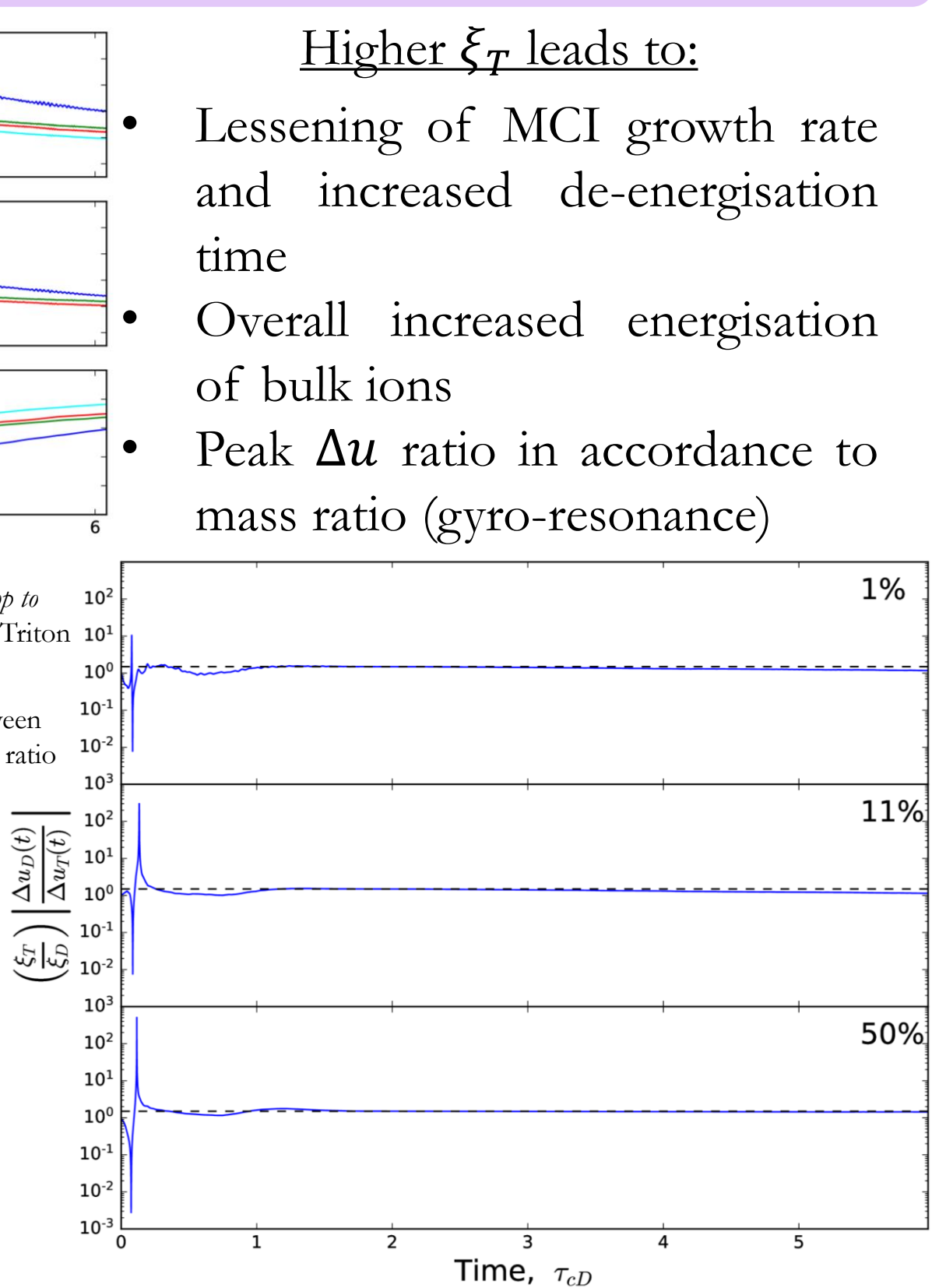


Fig. 6 (above) Change in energy densities per ionic species (top to bottom) of deuterons, tritons and alpha-particles through time. Triton concentration as labelled.

Fig. 7 (right) Change in energy density per-particle ratio between the deuterons and tritons, through time, with the inverse mass ratio plotted as a dashed grey line.

By assuming both DT species reach gyro-resonance through Larmor radii matching [7], one derives the ratio between their change in energy densities per-particle as the inverse of their mass ratios, Fig. 7.



Higher  $\xi_T$  leads to:

- Lessening of MCI growth rate and increased de-energisation time
- Overall increased energisation of bulk ions
- Peak  $\Delta u$  ratio in accordance to mass ratio (gyro-resonance)

## Conclusions

- First principles simulations of ICE spectra with tritium concentrations in the range 0% to 50% show best agreement with JET 26148 ICE when concentration = 11%, which coincides with the actual experimental value
- Preferential driving of shorter and slower plasma waves
- An increase in the magnitude of energy transfer from the alpha-particles to the DT bulk through slower growing MCI
- Frequency offset following a linear relation w.r.t  $\xi_T$ , eq. (3)
- Gyro-resonance between DT species, Fig. (7)